

NUMERICAL MODELLING OF THERMAL SPALLATION OF ROCK

Timo Saksala

Laboratory of Civil Engineering, Tampere University of Technology, P.O.Box 600, 33101 Tampere, Finland, timo.saksala@tut.fi, <http://www.tut.fi/en/research/research-fields/civil-engineering/>

Keywords: Thermal spallation, rock fracture, embedded discontinuity, finite elements

Abstract. This paper presents a numerical study on thermal spallation of rock. In the present context, thermal spallation refers to fragmentation of rock surface material when subjected to rapid external heating. For modelling the rock fracture in thermal spallation, an embedded discontinuity finite element approach is chosen. In the present implementation, a displacement discontinuity (crack) is embedded perpendicular to the first principal direction in a CST element upon violation of the Rankine criterion. The heating due to mechanical dissipation is neglected as insignificant in comparison to the external heat flux. Thereby, the underlying thermo-mechanical problem becomes uncoupled the only input from the thermal part to the mechanical part being thermal strains. This problem is solved with explicit time marching using the mass scaling to speed up the solution. A thermal spallation problem of a rock sample under axisymmetry is simulated as a numerical example. Different heat flux intensities are tested to demonstrate the capability of the method.

1 INTRODUCTION

Rapid heating of granitic rocks' surfaces causes them to disintegrate into disc-shaped chips called spalls (Kant and von Rohr, 2016). The principle of this phenomenon, called thermal spallation, is illustrated in Figure 1. Accordingly, the compressive stress state induced by an external heat shock generates new cracks in the rock due to mismatching elastic and thermal properties of the constituent minerals as well as further propagation of the existing cracks, e.g. by the wing crack mechanism. Further propagation of the cracks parallel to the rock surface leads to spalling, or ejection by buckling, of the fragments when cracks reach a critical length.

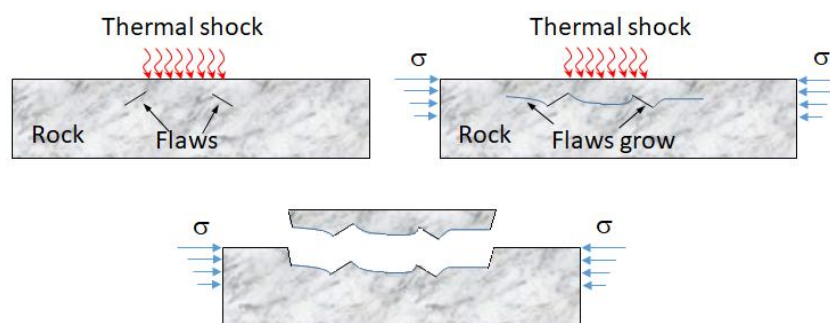


Figure 1: Principle of thermal spallation.

Thermal spallation, or weakening rock by heat shock in general, can be used in mining and excavation to assist (or even replace) traditional mechanical breakage. Therefore, it has been the topic of several numerical studies (Pressacco and Saksala, 2018; Walsh and Lomov, 2013; Whittles et al., 2003). In the present paper, a preliminary numerical study on thermal spallation of rock under axisymmetric conditions is presented.

For this end, a finite element based numerical method is described. The rock fracture model is based on the embedded discontinuity finite elements. In comparison to the external heat shock, the mechanical heating effects are insignificant. Therefore, the governing thermo-mechanical problem becomes uncoupled. Moreover, the material properties are assumed to be temperature independent in this preliminary study. A numerical example of heterogeneous granitic rock under a high intensity heat flux is solved under axisymmetric conditions in order to demonstrate the method.

2 THEORY OF THE NUMERICAL MODEL

A brief description of the modelling approach is given here. First, the finite element discretized equations of the thermal and mechanical parts of the problem are given. Then, the rock fracture model based on the embedded discontinuity finite elements is sketched. Finally, the time integration scheme of the uncoupled thermo-mechanical problem is outlined.

2.1 Finite element discretized heat equation and equation of motion

As mentioned above, the external heat flux in the thermal spallation problem is significantly larger than the heat generation due to mechanical response. Therefore, the coupling term involving the mechanical heating effects in the heat equation can be ignored. This being the case, the finite element discretized heat (balance) equation becomes

$$\mathbf{C}\dot{\boldsymbol{\theta}} + \mathbf{K}_0\boldsymbol{\theta} - \mathbf{f}_0 = \mathbf{0} \quad (1)$$

where \mathbf{C} , \mathbf{K}_0 , and \mathbf{f}_0 are the capacitance matrix, the conductivity matrix, and the external

force, respectively, defined as

$$\mathbf{C} = \int_V \rho c \mathbf{N}_\theta^T \mathbf{N}_\theta dV, \quad \mathbf{K}_\theta = \int_V k \mathbf{B}_\theta^T \mathbf{B}_\theta dV, \quad \mathbf{f}_\theta = - \int_A q_n \mathbf{N}_\theta^T dA \quad (2)$$

where ρ is the density, c is the specific heat capacity, θ is the temperature, \mathbf{N}_θ is the temperature interpolation matrix, k is the conductivity, q_n is the normal component of the heat flux, and \mathbf{B}_θ is the gradient of \mathbf{N}_θ . Generally, the specific heat capacity and conductivity depend on temperature but this dependency is neglected in this study.

The mechanical part of the thermal spallation problem is governed by the equation of motion, which is written as follows in the discretized form:

$$\mathbf{M}\ddot{\mathbf{u}} + \mathbf{f}_{\text{int}} = \mathbf{f}_{\text{ext}}, \quad \mathbf{f}_{\text{int}} = \mathbf{A}_{k=1}^{N_e} \int_{V_e} \mathbf{B}_u^T \boldsymbol{\sigma} dV \quad (3)$$

where \mathbf{M} is the mass matrix, \mathbf{u} is the displacement vector, $\boldsymbol{\sigma}$ is the stress matrix, \mathbf{f}_{ext} , \mathbf{f}_{int} are the external and internal force vectors, respectively, \mathbf{B}_u is the kinematic operator matrix, and \mathbf{A} is the standard finite element assembly operator.

2.2 Embedded discontinuity finite element model for rock

The constitutive model for rock employed here is based on the embedded discontinuity concept, which is an element based enrichment technique, in contrast to the extended finite element method, which is a nodal based enrichment technique. Accordingly, upon reaching an elastic limit in a finite element, e.g. tensile strength, a discontinuity line (surface in 3D) is embedded inside the element. In the present version, the Rankine criterion is used to indicate cracking and the discontinuity is oriented orthogonal to the first principal direction. A brief summary of the model originally presented by Saksala et al. (2015) is given here.

When a displacement discontinuity (crack) is embedded in a CST (constant strain triangle) element, the displacement and strain fields can be decomposed as

$$\mathbf{u} = N_i \mathbf{u}_i^e + (H_{\Gamma_d} - \varphi) \boldsymbol{\alpha}_d, \quad \boldsymbol{\varepsilon} = \nabla N_i \otimes \mathbf{u}_i^e - \nabla \varphi \otimes \boldsymbol{\alpha}_d$$

$$\nabla \varphi = \arg \left(\max_{k=1,2} \frac{|\sum_{i=1}^k \nabla N_i \cdot \mathbf{n}|}{\|\sum_{i=1}^k \nabla N_i\|} \right) \quad (4)$$

where $\boldsymbol{\alpha}_d$ is the displacement jump vector, N_i and \mathbf{u}_i^e are the standard interpolation function and displacement vector at node i (summation applies on repeated i), and H_{Γ_d} is the Heaviside function at discontinuity Γ_d with normal \mathbf{n} . Finally, φ is a function that restricts the effect of the displacement jump within the corresponding finite element so that the essential boundary conditions remain unaffected. It should also be mentioned that the gradient of the displacement jump is assumed zero here, i.e. constant mode I and II discontinuity is adopted. Equation (4) specifies also how function φ is selected from among the nodal interpolants.

A bi-surface, plasticity inspired model was developed in Saksala et al. (2015) for solving the displacement jump vector and the traction updates, as well as to control the softening behavior at the discontinuity. The components of this model are

$$\begin{aligned}
\phi_t(\mathbf{t}_{\Gamma_d}, \kappa, \dot{\kappa}) &= \mathbf{n} \cdot \mathbf{t}_{\Gamma_d} - (\sigma_t + q(\kappa, \dot{\kappa})), & \phi_s(\mathbf{t}_{\Gamma_d}, \kappa, \dot{\kappa}) &= |\mathbf{m} \cdot \mathbf{t}_{\Gamma_d}| - (\sigma_s + \frac{\sigma_s}{\sigma_t} q(\kappa, \dot{\kappa})) \\
\dot{\mathbf{a}}_d &= \dot{\mathbf{a}}_I + \dot{\mathbf{a}}_{II} = \dot{\lambda}_t \frac{\partial \phi_t}{\partial \mathbf{t}_{\Gamma_d}} + \dot{\lambda}_s \frac{\partial \phi_s}{\partial \mathbf{t}_{\Gamma_d}} \\
\dot{\mathbf{t}}_{\Gamma_d} &= -\mathbf{E} : (\nabla \varphi \otimes \dot{\mathbf{a}}_d) \cdot \mathbf{n}, & \dot{\kappa} &= -\dot{\lambda}_t \frac{\partial \phi_t}{\partial q} - \dot{\lambda}_s \frac{\partial \phi_s}{\partial q} \\
q &= h\kappa + s\dot{\kappa}, & h &= -g\sigma_t \exp(-g\kappa) \\
\dot{\lambda}_i &\geq 0, & \phi_i &\leq 0, & \dot{\lambda}_i \phi_i &= 0, & i &= t, s
\end{aligned} \tag{5}$$

where ϕ_t and ϕ_s are the tension (mode I) and shear (mode II) loading functions, respectively, $\kappa, \dot{\kappa}$ are the internal variable and its rate, \mathbf{m} is the crack tangent vector, σ_t and σ_s are elastic limits in tension and shear, respectively, $\mathbf{a}_I, \mathbf{a}_{II}$ are the mode I and II crack opening vectors, \mathbf{E} is the elasticity tensor, $\dot{\lambda}_t, \dot{\lambda}_s$ are the mode I and II opening increments, respectively, h is the softening modulus, and s is the constant viscosity modulus. The softening slope parameter g is defined by the mode I fracture energy G_{Ic} by $g = \sigma_t/G_{Ic}$.

The problem defined by model (5), i.e. the traction and internal variables update, can be solved with the standard algorithms of multisurface plasticity. After this, a new stress is calculated by

$$\boldsymbol{\sigma} = \mathbf{E} : (\boldsymbol{\varepsilon}_{tot} - \nabla \varphi \otimes \mathbf{a}_d - \boldsymbol{\varepsilon}_\theta), \quad \boldsymbol{\varepsilon}_\theta = \alpha \Delta \theta \mathbf{I} \tag{6}$$

where $\boldsymbol{\varepsilon}_{tot}$ and $\boldsymbol{\varepsilon}_\theta$ are the total and thermal strain tensor, respectively, α is the thermal expansion coefficient, $\Delta \theta$ is the temperature difference, and \mathbf{I} is the identity tensor.

2.3 Explicit scheme for solving the uncoupled thermo-mechanical problem

As already mentioned, the uncoupled thermo-mechanical problem governing the thermal spallation is solved with explicit time marching. Euler method is employed here leading to following equation for the new temperature $\boldsymbol{\theta}_{n+1}$:

$$\mathbf{C}_n \boldsymbol{\theta}_{n+1} = (\mathbf{C}_n - \Delta t \mathbf{K}_{\theta,n}) \boldsymbol{\theta}_n + \Delta t \mathbf{f}_{\theta,n} \tag{7}$$

The mechanical update is performed as follows:

$$\begin{aligned}
\mathbf{M} \ddot{\mathbf{u}}_t + \mathbf{f}_{int,t} &= \mathbf{f}_{ext,t} \rightarrow \ddot{\mathbf{u}}_t \\
\dot{\mathbf{u}}_{n+1} &= \dot{\mathbf{u}}_n + \Delta t \ddot{\mathbf{u}}_t, & \mathbf{u}_{n+1} &= \mathbf{u}_n + \Delta t \dot{\mathbf{u}}_{n+1}
\end{aligned} \tag{8}$$

Now, the solution procedure for the uncoupled thermo-mechanical problem is as follows. First, the temperature is solved by equation (7). Then, the stress and internal variable updates are performed through equations (5) and (6). Finally, the mechanical response is advanced by solving (8).

3 NUMERICAL EXAMPLE

A problem thermal spallation of rock is simulated here in order to test the numerical method presented above. Numerical rock is assumed to be heterogeneous with three different minerals (Quartz, Feldspar, and Biotite). The heterogeneity is described as follows. First, the element numbers are assigned integers from 1 to 3 corresponding to the percentage of the

minerals in rock. For example, if the real rock has 33 % of Quartz, then 33 % percent of the elements in the mesh are designated as Quartz. Then, the sets representing different minerals are randomly mapped into the mesh resulting in a mesoscopic description of heterogeneity. The material and model properties for minerals are in Table 1.

Parameter	Quartz	Feldspar	Biotite
%	33	50	17
ρ [kg/m ³]	2616	2616	2616
E [GPa]	80	60	20
ν	0.17	0.29	0.20
σ_t [MPa]	10	8	7
σ_s [MPa]	50	50	50
G_{Ic} [J/m ²]	40	40	28
α [1/K]	1.60E-5	0.75E-5	1.21E-5
k [W/mK]	4.94	2.34	3.14
c [J/kgK]	731	730	770

Table 1: Material and model parameter for typical minerals found in granitic rocks

Due to the vastly differing time scales, and hence the critical time steps of the explicit schemes (7) and (8), of the thermal and mechanical problems, mass scaling is used to speed up the solution in time. The present problem turned out to be especially suitable for extreme mass scaling: numerical tests revealed that the response remained virtually identical even when the density for the mechanical part of the problem was 10000-fold resulting in a critical time step of 100 times larger than that with the original density.

The boundary conditions and the numerical rock are shown in Figure 2.

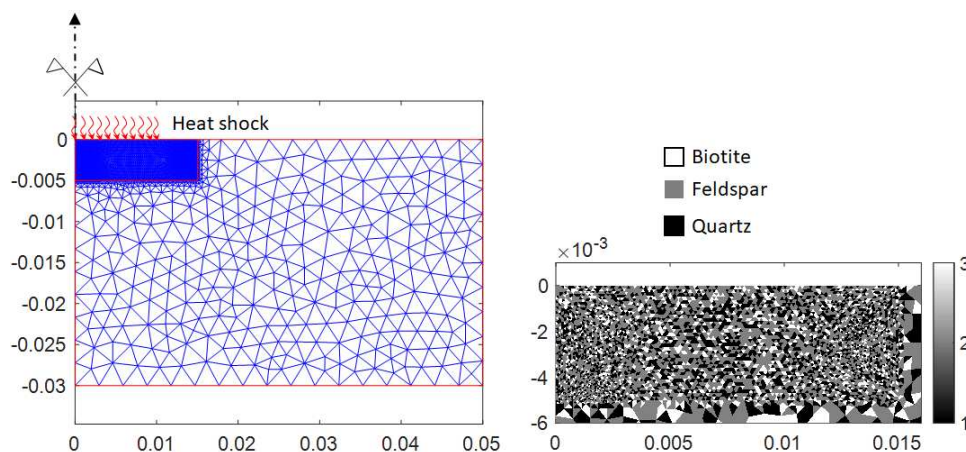


Figure 2: The CST mesh (7961 elements, the unit of the dimensions is m), boundary conditions, and the numerical rock mineral structure.

The average element size in the area affected by the heat shock is about 0.1 mm leading to a critical time step of order 1E-9 s. Therefore, the mass-scaled time step is of order 1E-7 s requiring quite short practical analysis times. Here, a heating time of 10 ms is set, and the intensity of the thermal shock needs thus be very high in order to cause spalling. Figure 3 shows simulation results with constant heat flux $q_n = 5E6$ J/m².

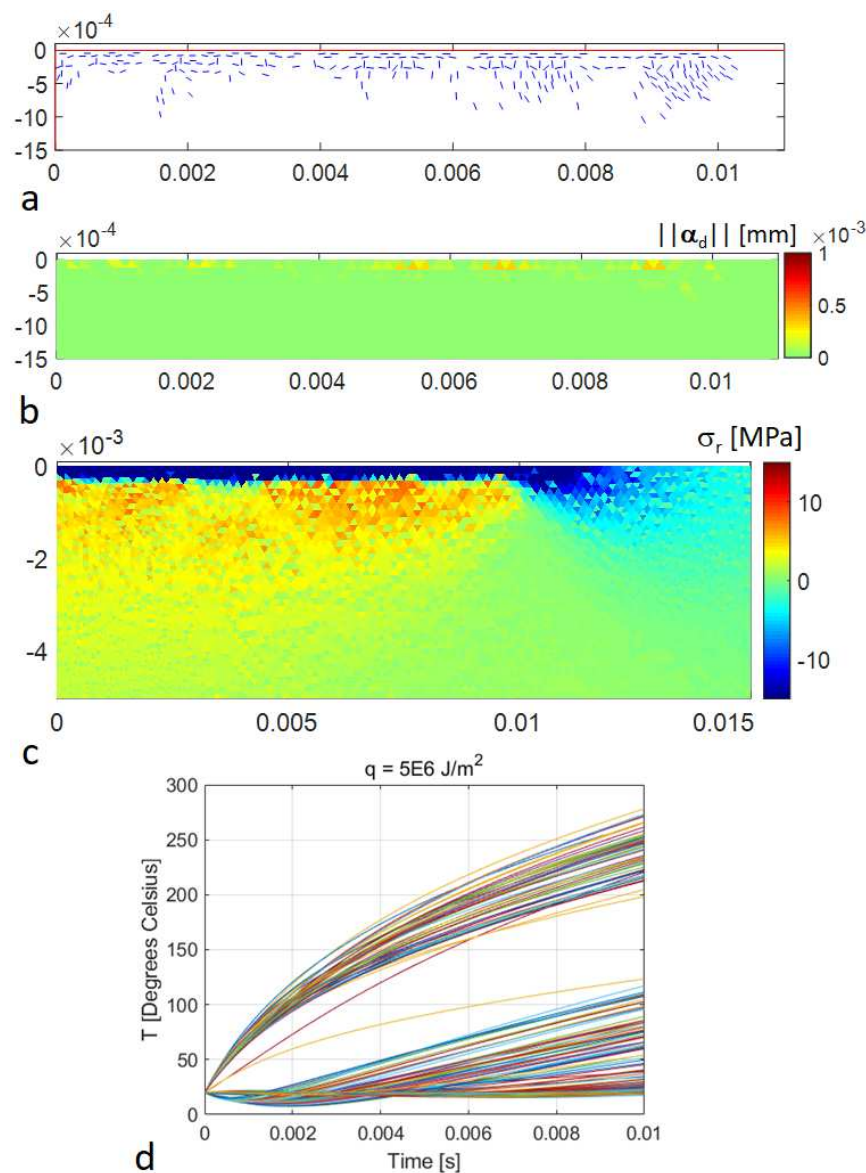


Figure 3: Simulation results for the thermal spallation of rock under constant heat flux $q_n = 5E6 \text{ J/m}^2$: the crack orientations (a), the magnitude of crack opening vectors (b), the radial stress distribution (c) at the end of simulation, and the temperature evolution at all nodes of the rock sample (d).

According to the results in Figure 3a, the induced cracks are oriented parallel to the surface right beneath the heat shock where the radial stress is compressive (Figure 3c). Deeper in the rock, where the radial stress is tensile, the crack orientation changes to more perpendicular to the surface. The nodal temperatures at the end of simulation are shown in Figure 3d. At the surface nodes directly exposed to the heat flux, the temperatures vary between 200 and 270 degrees Celsius, which is not enough to cause spalling as the maximum opening of the cracks is less than 0.001 mm, see Figure 3b.

Next, the same simulation is carried out with a stronger heat shock. The results are shown in Figure 4.

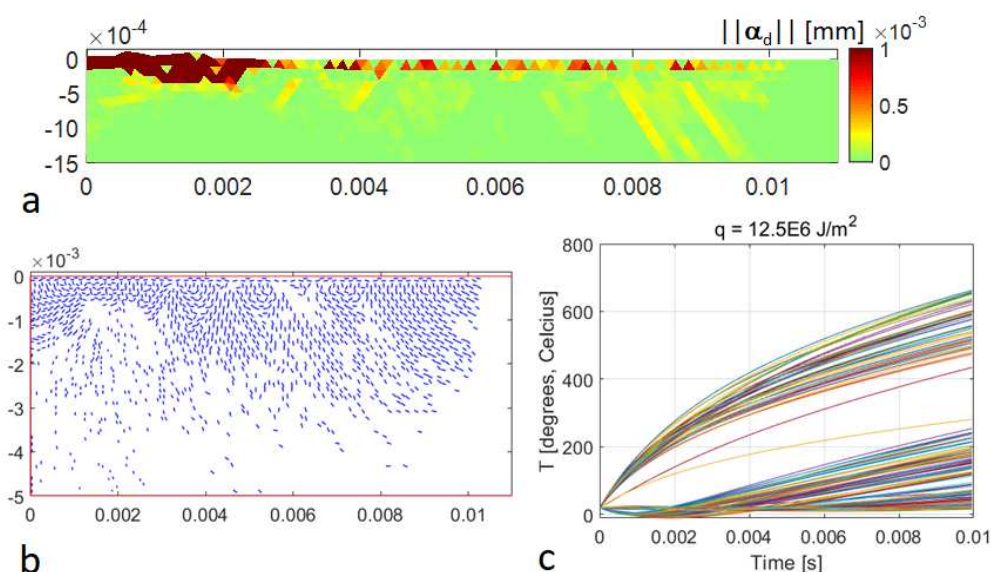


Figure 4: Simulation results for the thermal spallation of rock under a constant heat flux $q_n = 12.5E6 \text{ J/m}^2$: the magnitude of crack opening vectors (a), the crack orientations (b) at the end of simulation, and the temperature evolution at all nodes of the rock sample (c).

With the stronger heat shock, the number of induced cracks is much higher and their magnitude of opening close to the rock surface is substantially larger than with the weaker heat shock. Indeed, the maximum value of α_d at cracks close to the symmetry axis exceeds 0.1 mm in many elements, see Figure 4a. It should be noted that the deformations are not magnified. The corresponding temperatures at the surface nodes range from 450 to 650 degrees Celsius (Figure 4c). According to the experimental study by Kant and von Rohr (2016), typical temperatures required for spallation to occur in granitic rocks, range from 550 to 650 degrees Celsius. Therefore, spallation is predicted by the simulation results in Figure 4.

4 CONCLUSIONS

A relatively simple numerical method to model thermal spallation of rock based on embedded discontinuity finite elements was presented. The mechanical heating effects were ignored as insignificant compared to the external heat shock. Thereby, the finite element discretized uncoupled thermo-mechanical problem was solved with explicit time marching. The mechanical part of the problem was particularly amenable to mass scaling allowing the mass to be scaled even to 10000-fold without observable differences in the results. The simulation results were encouraging in the sense that the predicted temperatures, at which the spallation of granitic rock occurs, were in reasonable agreement with the experiments.

ACKNOWLEDGEMENTS

This research was funded by Academy of Finland under Grant number 298345.

REFERENCES

Kant, M.A., von Rohr, P.R., Minimal required boundary conditions for the thermal spallation process of granitic rocks. *International Journal of Rock Mechanics & Mining Sciences*, vol. 84, pp. 177–186, 2016.

- Pressacco, M., Saksala, T., Numerical modelling of fracture process in thermal shock weakened rock. In: Litvinenko v. (Ed.) Proceedings of the 2018 European Rock Mechanics Symposium (EUROCK2018: Geomechanics and Geodynamics of Rock Masses), Saint Petersburg, Russia, 22-26 May, 2018. Vol 1, pp. 883-888.
- Saksala, T., Brancherie, D., Harari, I., Ibrahimbegovic, A. Combined continuum damage-embedded discontinuity model for explicit dynamic fracture analyses of quasi-brittle materials. *International Journal for Numerical Methods in Engineering*, vol. 101, pp. 230–250, 2015.
- Walsh, S. D. C., Lomov I.N., Micromechanical modeling of thermal spallation in granitic rock. *International Journal of Heat and Mass Transfer*, vol. 65, pp. 366–373, 2013.
- Whittles, D.N., Kingman S.W., Reddish, D.J., Application of numerical modelling for prediction of the influence of power density on microwave-assisted breakage. *International Journal of Mineral Processing*, vol. 68, pp. 71–91, 2003.